doi: 10.13133/2280-6148/18620 *Journal of Mediterranean Earth Sciences 16 (2024), 69-85*

J M E S **Journal of Mediterranean Earth Sciences**

Assessing the sensitivity of land cover (C factor) to water erosion in the Ksob watershed, central Algeria

Fouad Sakhraoui [1,*], Mahmoud Hasbaia [2]

[1] *Research Laboratory of Applied Hydraulics and Environment (LRHAE), Faculty of Technology, University of Bejaia, 06000 Bejaia, Algeria*

[2] *CEHSD Laboratory, University of M'sila, 28000 M'sila, Algeria*

* *Corresponding author: fouad.sakhraoui@univ-bejaia.dz*

ABSTRACT - Water erosion is a critical environmental and economic issue, causing soil fertility loss and land degradation, recognized globally as one of the most severe natural threats. Algeria's high topography, diverse vegetation, and heavy rainfall make it particularly vulnerable to water erosion. This study employs the Revised Universal Soil Loss Equation (RUSLE) model integrated with geographic information systems (GIS) to analyze the Ksob watershed from 2017 to 2023. It examines seasonal and interannual variations in the vegetation cover management (C factor), assesses the impact of changes in land use and land cover (LULC) on soil erosion, and investigates the relationship between the C factor and soil erosion. Findings indicate significant soil loss variations due to changes in vegetation cover: reduced vegetation increases erosion rates, while dense vegetation mitigates them. Despite cultivated land expanding from 25.39% to 35.84% during the study period, the average annual soil loss rose by 11.21%, from 9.06 t ha^{-1} yr^{-1} to 10.08 t ha^{-1} yr^{-1}. Spatial analysis revealed that low erosion classes covered approximately 70% of the area, with summer and autumn identified as the most erosive seasons, showing rates over 10 t ha^{-1} yr^{-1}. The study confirms a strong relationship between vegetation cover and erosion rate.

Keywords: Algeria; C factor; GIS, LULC; RUSLE; water erosion.

Submitted: 27 August 2024 - Accepted: 17 November 2024

1. INTRODUCTION

Soil erosion presents a substantial environmental and economic challenge, leading to detrimental impacts such as water quality decline, soil fertility loss, and land degradation (Mahleb et al., 2022). Globally, it is recognized as one of the most severe natural threats (Gwapedza et al., 2021). This issue is especially acute in regions across Africa, Latin America and Asia, as highlighted by the Food and Agriculture Organization (FAO) (Nourizadeh et al., 2024).

Algeria is particularly susceptible to water erosion, which affects an area of 10 million hectares per year (Mazour and Roose, 2002) due to the country's high topography, varied vegetation cover, and heavy rainfall. Human actions including urbanization, infrastructure development, and deforestation aggravate the effects of soil loss on the environment and the economy (Dechen et al., 2015; Bollati et al., 2016; Polidoro et al., 2021). However, water remains the main driving force behind erosion (Wang et al., 2018).

The rate of soil erosion is influenced by various factors, including human activities, land management practices, population growth, climate change, and changes in land use and land cover (LULC) (Ochoa et al., 2016; Rodrigues and Costa, 2021; Valkanou et al., 2022). Changes in LULC are particularly significant for soil erosion, and having access to accurate maps of these changes is crucial for identifying critical erosion points and ensuring sustainable soil management (Chaves et al., 2020).

More accurate modeling and estimation of soil erosion rates are now possible thanks to developments in informatics technology, particularly remote sensing and geographic information systems (GIS), as well as access to high-quality geospatial data (Belasri and Lakhouili, 2016; Tadesse et al., 2017; Negese et al., 2021). Numerous models and approaches for assessing soil erosion have been developed by the scientific community, including the Universal Soil Loss Equation (USLE) (Wischmeier and Smith, 1965, 1978), the Revised Universal Soil Loss Equation (RUSLE) (Renard et al., 1997), the Soil and Water Assessment Tool (SWAT) (Arnold et al., 1998), and

the European Soil Erosion Model (EuroSEM) (Morgan et al., 1998). Due to their simplicity and low computational requirements, empirical models like RUSLE are among the most widely used across various regions, particularly in Algeria (Sahli et al., 2019) and in Mediterranean and European areas (Van Rompaey et al., 2001; Fernández and Vega, 2016). These models, whether empirical, conceptual, or physical, allow for the quantification of erosion while providing the flexibility needed to address the specific demands of regional studies.

The RUSLE model integrates five critical factors: rainfall erosivity (R factor), slope length and steepness (LS factor), soil erodibility (K factor), vegetation cover management (C factor), and conservation practices (P factor). RUSLE is known for its straightforward structure, ease of comprehension, and adaptability to large-scale applications (Koirala et al., 2019; Santana et al., 2021; Sifi et al., 2024). It can also assess erosion in a matrix format (Phinzi and Ngetar, 2019). However, its limitations include a primary focus on rill and inter-rill erosion, while other forms of erosion, such as lateral erosion of river channels, are not accounted for (Vandekerckhove et al., 1998; Xu et al., 2012).

Considering the diverse factors influencing soil erosion, this study aims to achieve several specific objectives: (1) to analyze seasonal and interannual variations in C factor in the Ksob watershed over the period 2017 to 2023, (2) to examine the impact of changes in LULC on the estimation of soil erosion, and (3) to investigate the possibility of finding a significant relationship between C factor and soil erosion rates. By achieving these objectives, the study hopes to provide practical recommendations for sustainable soil management in the Ksob watershed, thus contributing to reducing the environmental and economic impacts of soil erosion in this vulnerable region.

2. MATERIALS AND METHODS

2.1. STUDY AREA

The Ksob watershed in central Algeria is a sub-basin of the extensive Hodna basin. The watershed covers an area of 1418 km^2, with a broad plateau in the center and very steep terrain in the mountains, ranging in altitude from 595 m to 1903 m (Fig. 1). It lies between 35°48' and 36°09' north latitude and 4°28' and 5°09' east longitude.

The Gravelius compactness coefficient of the watershed is 1.59, and its perimeter measures 214 km. It experiences an average rainfall of 303 mm, characterized by spatio-temporal irregularity and high intensity. All morphometric parameters and hydro-climatological analyses of the watershed are described in previous works (Sakhraoui and Hasbaia, 2023).

The slope map (Fig. 2), generated from a Digital Elevation Model (DEM) with a 10-meter spatial resolution obtained from Sentinel-1 satellite data (accessible at https://scihub.copernicus.eu/), illustrates that 76.58% of the total area consists of low and very low slopes (0-10%) (refer to table 1). Moderate slopes cover 12.54% of the land area. Steep slopes ranging from 12.5% to 25% are predominantly located in the south-southeastern part, occupying 10.30% of the watershed area and posing a high risk of erosion.

The central part of the basin is primarily dedicated to agriculture, with cereals covering approximately 70% of the area (Benkadja et al., 2015). Matorral and grasslands occupy 25% of the land, and forests cover approximately 5%. These land use patterns render the watershed highly vulnerable to soil erosion, especially during heavy rainfall events.

2.2. DATA SOURCE AND RUSLE MODEL

A systematic approach is essential for accurately understanding and predicting the processes and factors

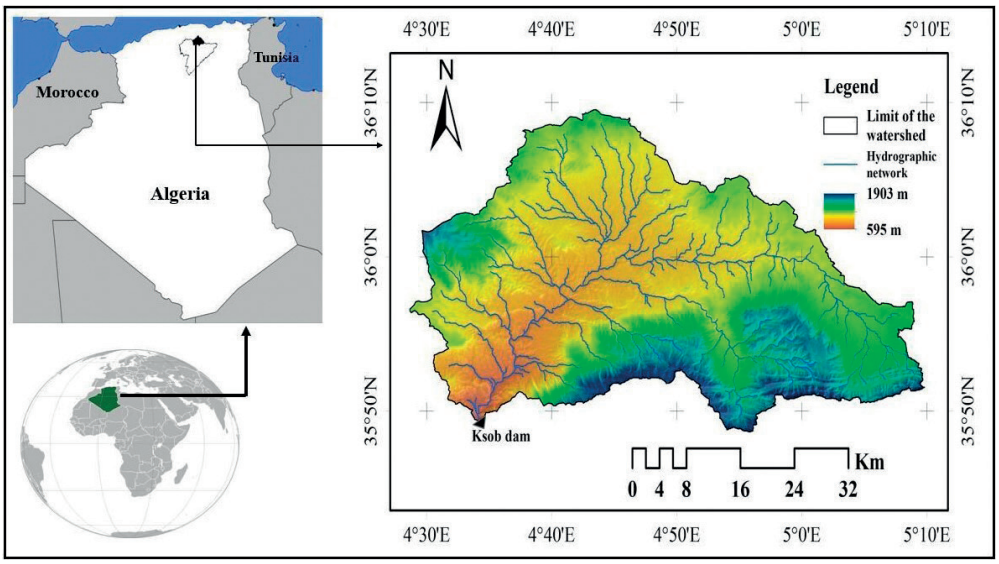

Fig. 1 - Study area locations.

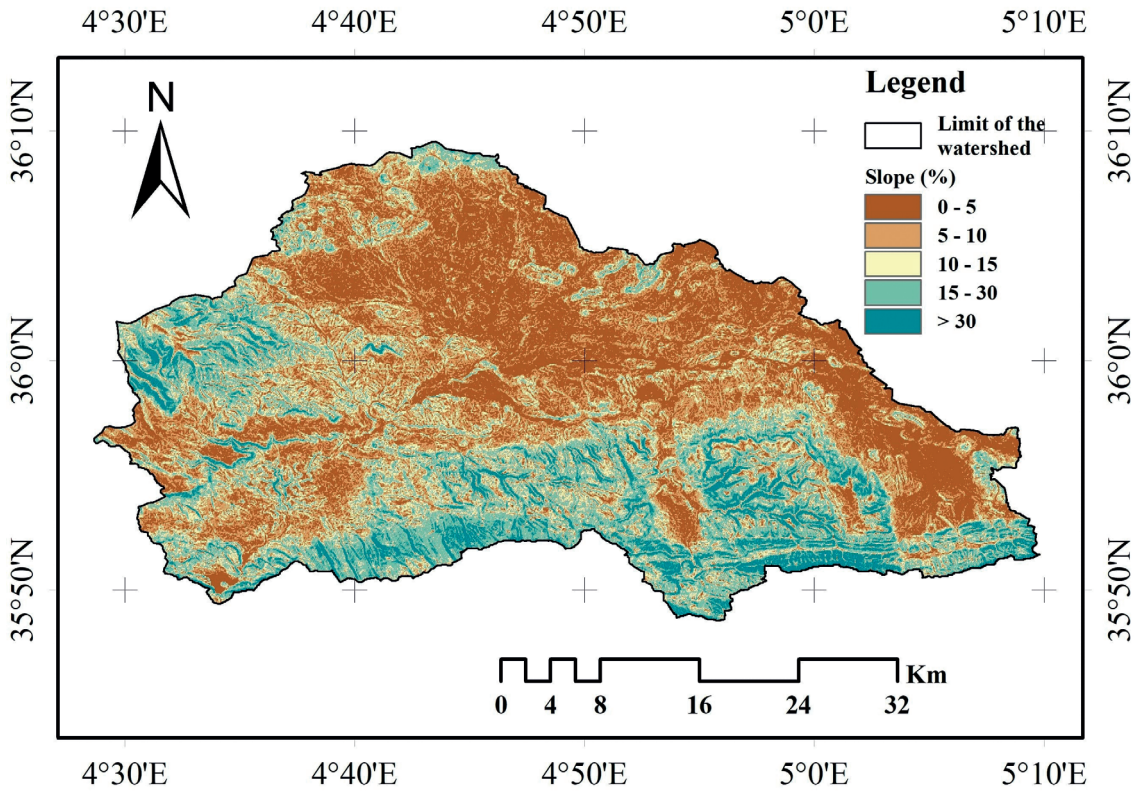

Fig. 2 - Slop map of the Ksob watershed.

Tab. 1 - Classes of slope in the Ksob watershed.

Designation	Classes of slope (%)	Area (km²)	Area (%)
Very low slopes	0-5	580.28	40.92
Low slopes	5-10	505.60	35.66
Moderate slopes	10-15	177.83	12.54
High slopes	15-30	146.02	10.30
Very high slopes	> 30	8.27	0.58
	Total	1418	100

driving soil erosion. In this research, the RUSLE model was applied to estimate soil erosion rates in the Ksob watershed. The RUSLE equation, as outlined by Renard et al. (1997), was utilized to effectively integrate these variables for precise erosion assessment.

$$A=R\cdot K\cdot LS\cdot C\cdot P \quad (1)$$

Where A represents the average annual soil loss (t ha^{-1} yr^{-1}), R is the rainfall erosivity factor (MJ.mm ha^{-1} h^{-1} yr^{-1}), K is the soil erodibility factor (t h MJ^{-1} mm^{-1}), LS indicates the slope length and steepness factor (dimensionless), C is the crop and management factor (dimensionless), and P represents the conservation practice factor (dimensionless). The implementation of the RUSLE model methodology involves employing GIS tools to streamline the process and generate maps at a spatial resolution suitable for the study, set at 10 meters. ArcGIS 10.2 software was utilized to create soil erosion rate maps for the Ksob watershed (Fig. 3).

2.2.1. Rainfall erosivity (R factor)

The R factor quantifies the erosive potential of rainfall in causing water erosion. Various methods exist to estimate the R factor, chosen based on data availability and specific study area requirements. In the Ksob watershed, the Diodato (2004, 2005) formula was employed, utilizing parameters such as average annual rainfall (P), longitude of the station (L), and annual maximum daily rainfall (d). This formula was selected due to its suitability demonstrated in prior studies (Sakhraoui and Hasbaia, 2023).

Rainfall data from rain gauging stations within and around the Ksob watershed, collected by the National Agency for Hydraulic Resources (NAHR), spans the years 1975 to 2015. The Diodato (2004, 2005) model, which is used to estimate rainfall erosivity (R factor), is defined by the following equation:

$$R=b_0\cdot P\cdot\sqrt{d}\cdot(\alpha+b_1\cdot L) \quad (2)$$

Where P represents the average annual rainfall in mm, d is the annual maximum daily rainfall in mm, and L denotes the site's longitude in degrees. The constants are given as b_0=0.117 MJ mm ha^{-1} h^{-1}, α=2.00 $day^{0.5}$ $mm^{-0.5}$

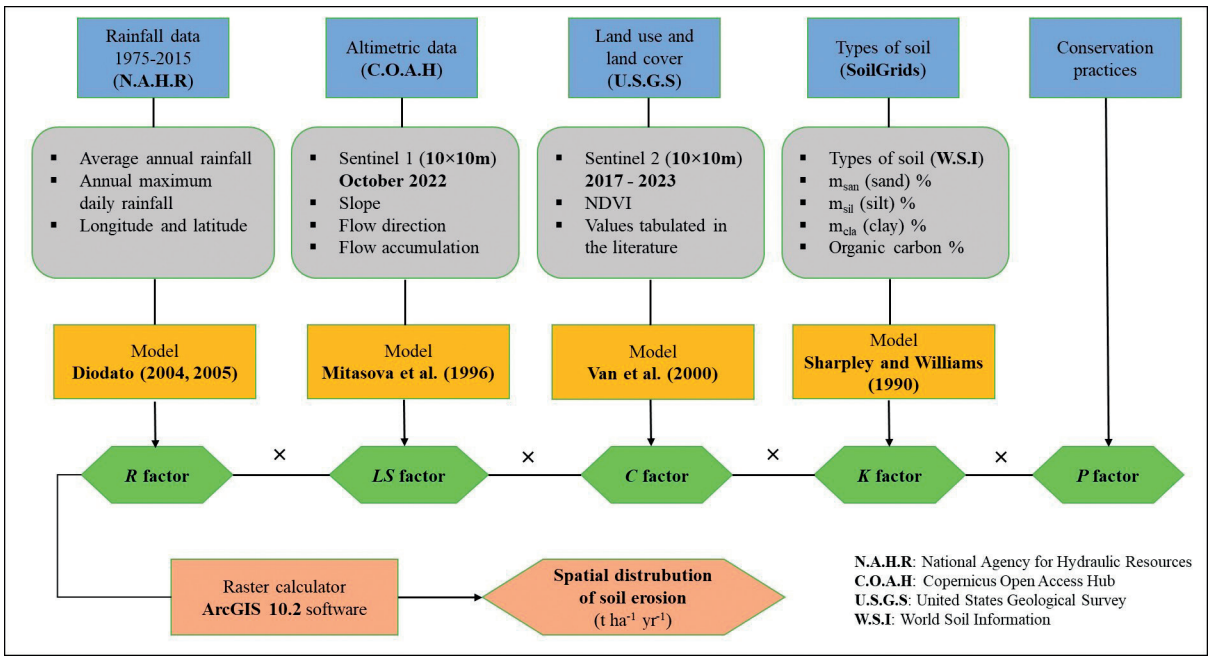

Fig. 3 - Data Sources and RUSLE model for soil erosion estimation in the Ksob Watershed.

and b_1=-0.015 day$^{0.5}$ mm$^{-1.5}$. The R factor values were computed individually for each station and spatially interpolated across the entire basin using inverse distance weighting (IDW). This method was identified as optimal for interpolating various climatic variables and has been widely applied in the literature (Gayen et al., 2020; Degife et al., 2021; Sifi et al., 2024).

2.2.2. Soil erodibility (K factor)

The K factor plays an important role in estimating soil loss and guiding soil conservation efforts. It reflects the soil's inherent susceptibility to erosion, which is influenced by its physical properties and characteristics (Chang et al., 2016). This factor is calculated using four key parameters: the soil's sand, silt, and clay percentages, as well as its organic matter content. These parameters collectively define the erodibility of the soil, capturing how easily it can be detached and transported by erosive forces.

In this research, the K factor data were obtained from SoilGrids, a global soil information database provided by ISRIC World Soil Information (available at https://www.isric.org/explore/soilgrids). The data used have a spatial resolution of 250 meters and pertain to the top 0-0.15 m soil layer. This dataset has been utilized in various studies by researchers investigating soil erosion dynamics and conservation practices (Baskan, 2021; Sourn et al., 2022).

The equation (3), formulated by Sharpley and Williams (1990), has been applied in studies conducted by Neitsch et al. (2011), Al Rammahi and Khassaf (2018), and Sourn et al. (2022), to estimate this factor.

$$K=f_{sand}\cdot f_{silt\text{-}clay}\cdot f_{oc}\cdot f_{hisand} \quad (3)$$

Where: f_{sand} is a parameter that reduces the K value for soils with coarse sand content, $f_{silt\text{-}clay}$ indicates a lower soil erodibility parameter for soils with high clay content, f_{oc} moderates K values for soils containing organic carbon, and f_{hisand} decreases K values for soils with very high sand content.

$$f_{sand} = \{0.2 + 0.3 \times \exp\left[-0.0256 \times m_{san} \times \left(1 - \frac{m_{sil}}{100}\right)\right]\} \quad (4)$$

$$f_{silt-clay} = \left(\frac{m_{sil}}{m_{cla} + m_{sil}}\right)^{0.3} \quad (5)$$

$$f_{oc} = \left(1 - \frac{0.25 \times m_{oc}}{m_{oc} + \exp[3.72 - (2.95 \times m_{oc})]}\right) \quad (6)$$

$$f_{hisand} = \{1 - \frac{0.7 \times \left(1 - \frac{m_{san}}{100}\right)}{\left(1 - \frac{m_{san}}{100}\right) + \exp\left[-5.51 + 22.9 \times \left(1 - \frac{m_{san}}{100}\right)\right]} \quad (7)$$

Where the variables m_{sil}, m_{san}, m_{cla}, and m_{oc} respectively indicate the percentage of silt, sand, clay, and organic carbon content in the soil layer.

2.2.3. Topographic factor (LS factor)

The LS factor assesses the combined influence of slope length (L) and slope steepness (S) on soil erosion dynamics (Belkendil et al., 2018). It is crucial in evaluating and modeling soil erosion susceptibility, as it considers the impact of terrain features on the erosion process (Vergari et al., 2019).

Equation (8) developed by Mitasova et al. (1996) for estimating the LS factor has been widely adopted in the literature, including studies by researchers such as Atoma et al. (2020), and Damian and Rafał (2023).

$$LS = (\text{Flow accumulation} \times \frac{\text{grid size}}{22.13})^{0.4} \times (\sin(\text{slope}) \times \frac{0.01745}{0.09})^{1.4} \quad 8)$$

Where sin (slope) is the sin of the slope degree value.

The topographic parameters required for applying the aforementioned equation were obtained using a DEM derived from "Sentinel 1," developed by the European Space Agency (ESA). This DEM, with a spatial resolution of 10 meters, was accessed through the Copernicus Open Access Hub (https://scihub.copernicus.eu/) in October 2022.

2.2.4. Crop management (C factor)

The C factor presents the cover and cultivation factor and describes the ratio of soil erosion of a randomly cultivated area to that of a plowed fallow (Wischmeier and Smith, 1978). it is probably the most complex factor of RUSLE and is the main focus of this study. The C factor is a dimensionless factor between 0 and 1, primarily depending on the percentage of plant cover and the growth phase (Renard et al., 1997).

In recent years, remote sensing and GIS methods have often been used to determine the C factor on a catchment scale. They are used for large areas and above all for different land use systems, and therefore often go beyond agriculture. Approaches such as Normalized Differenced Vegetation Index (NDVI) are used to infer vegetation cover and its evolution from satellite data (Puente et al., 2011; Liu et al., 2020; Singh et al., 2023).

The NDVI formula utilizes the near-infrared (NIR) and red (Red) spectral bands, as expressed below in equation (9):

$$\mathrm{NDVI} = \frac{\mathrm{NIB} - \mathrm{Red}}{\mathrm{NIB} + \mathrm{Red}} \quad (9)$$

NDVI values can vary from -1 to +1. The negative values are associated with surfaces such as water, snow, or clouds, which reflect more in the red band than in the near-infrared. Bare soils, which reflect similarly in both bands, typically produce NDVI values between 0 and 0.15. Vegetation cover yields positive NDVI values, generally ranging from 0.15 to 1.0, with denser vegetation resulting in higher NDVI values (Meusburger et al., 2010).

In this research, the C factor is assessed using equation (10) proposed by Van et al. (2000), a method that has been widely adopted by several researchers for its effectiveness in quantifying vegetation cover impacts on soil erosion (Durigon et al., 2014; Guerra et al., 2016; Macedo et al., 2021).

$$C = \exp^{\left[-\alpha\left(\frac{\mathrm{NDVI}}{\beta-\mathrm{NDVI}}\right)\right]} \quad (10)$$

Where the constants are given as α=2 and β=1 (Van et al., 2000).

The C factor and NDVI were computed seasonally (January, April, July, and October) for each year (2017 and 2023) using Sentinel-2 satellite images, which have a spatial resolution of 10 meters (sourced from the USGS, http://earthexplorer.usgs.gov/). This dataset provided historical LULC cover information, facilitating the analysis of land surface changes over time. To evaluate the influence of LULC on soil erosion, the C factor was calculated after NDVI acquisition, supported by a comprehensive literature review. C factor values for different land use categories were derived from authoritative sources such as Morgan (2005) and FAO (2012), utilizing values documented in the literature (Tab. 2). According to Lillesand and Kiefer (2000) state that image classification techniques are primarily designed to automatically categorize each pixel in an image into specific LULC classes.

2.2.5. Conservation support practice (P factor)

The P factor represents a conservation strategy that can influence soil erosion within a specific soil management context. By reducing runoff velocity, techniques such as terraces, contours, silt fences, and strip cropping reduce the potential for soil erosion (Wischmeier and Smith, 1978). This factor is dimensionless and ranges from 0 to 1, with 0 indicating no supportive practices (no erosion control) and 1 indicating the implementation of highly effective erosion control practices. In the study area, the absence of significant erosion control measures necessitated assigning a P factor value of 1 across the entire watershed.

2.3. ANNUAL EROSIVE POTENTIAL (A FACTOR)

Soil erosion in the watershed was classified according to the criteria established by Morgan (2005) and Gemechu et al. (2016), as detailed in table 3. The results of the classification were analyzed and compared with the Soil and Water Conservation Bulletin information.

The annual soil erosion potential (A factor) for the Ksob watershed is determined by multiplying the five parameter layers using ArcGIS 10.2.2 software. This

Tab. 2 - The *C* factor range for different LULC classes.

LULC class	Description	C factor range
Water	Areas covered by water, including rivers, lakes, reservoirs	0 - 0.05
Urban area	Areas characterized by high human activity, infrastructure, and built structures	0.05 - 0.1
Trees	Area encompassed natural forests, plantations, and other areas where trees are the predominant vegetation	0.1 - 0.2
Vegetations	Areas included croplands, pastures, and orchards	0.2 - 0.5
Rangland	Areas primarily covered by grasses, forbs, and shrubs, with minimal tree cover	0.5 - 0.9
Bare land	Areas with low or no vegetation cover	0.9 - 1

Tab. 3 - Soil erosion classes.

Soil erosion classes	Rang values (t ha^{-1} yr^{-1})
Very low	< 3
Low	3 - 10
Moderate	10 - 25
High	25 - 50
Very high	> 50

process generates the results in raster format (*.tiff), following the standard RUSLE equation.

3. RESULTS AND DISCUSSION

3.1. RAINFALL EROSIVITY (R FACTOR)

The R factor is a crucial parameter in the RUSLE model, quantifying the erosive power of rainfall in soil erosion modeling. The R factor was evaluated using the Diodato (2004, 2005) formula, which considers the distribution of annual maximum daily rainfall, average annual rainfall, and the station's longitude in degrees. This method provides a reliable estimate of the R factor. The rationale for selecting this estimation method is detailed in previous research by Sakhraoui and Hasbaia (2023).

As illustrated in figure 4, rainfall erosivity across the Ksob watershed varies from 252 to 504 MJ mm ha^{-1} h^{-1} yr^{-1}, with an average value of 413 MJ mm ha^{-1} h^{-1} yr^{-1}, as determined by data from various rainfall stations (Fig. 8). The areas with the highest R factor values, exceeding 400 MJ mm ha^{-1} h^{-1} yr^{-1}, account for more than 67% of the watershed and are primarily located in the central and eastern parts of the study area. These regions are characterized by elevated altitudes and exhibit an increasing gradient of rainfall aggressiveness from east to west. In contrast, the lowest R factor values are found in the western part of the watershed, an area marked by lowlands with a semi-arid climate and lower altitudes, covering less than 33% of the watershed. The range of R factor values observed in the Ksob watershed is consistent with findings from other regions in Algeria, such as the Wadi Mina watershed (Benchettouh et al., 2017) and the Soummam watershed (Sahli et al., 2019).

3.2. SOIL ERODIBILITY (K FACTOR)

The K factor indicates the soil's susceptibility to detachment and transportation by water, influenced by properties such as texture, structure, particle size, and organic matter content. In the Ksob watershed, the K factor was estimated using the Sharpley and Williams (1990) model, which considers soil composition and organic matter levels.

The spatial analysis identified five distinct soil categories (Tab. 4), with erodibility values ranging from 0.224 to 0.282 t h MJ^{-1} mm^{-1} across the watershed. The highest erodibility values were observed in the eastern

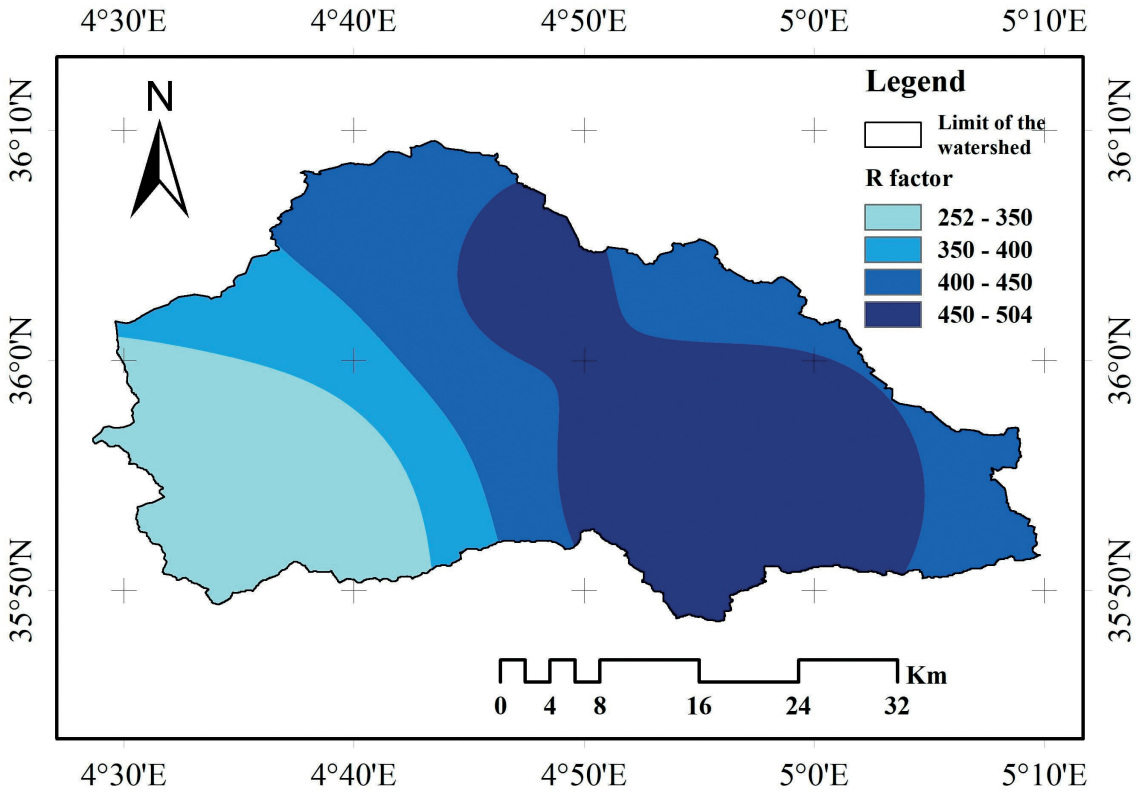

Fig. 4 - Spatial distribution of the rainfall erosivity factor (MJ mm ha^{-1} h^{-1} yr^{-1}).

Tab. 4 - *K* factor values of different soil types in the Ksob watershed (t h MJ^{-1} mm^{-1}).

Soil types	Sand topsoil (%)	Silt topsoil (%)	Clay topsoil (%)	Organic carbon (%)	f_{sand}	$f_{silt\text{-}clay}$	f_{oc}	f_{hisand}	*K* values	Area (km^2)	Area (%)
Calcic Cambisols	40.10	36.33	23.57	1.08	0.36	0.86	0.90	0.99	**0.277**	140.27	9.89
Calcic Cambisols	38.20	37.63	24.17	1.08	0.36	0.86	0.90	0.99	**0.282**	106.55	7.51
Haplic Xerosols	40.66	34.37	24.97	1.20	0.35	0.85	0.87	0.99	**0.261**	619.71	43.70
Lithosols	40.84	34.27	24.89	2.41	0.35	0.85	0.75	0.99	**0.224**	550.76	38.84
Calcic Yermosols	48.41	29.75	21.84	0.64	0.33	0.85	0.98	0.99	**0.269**	0.71	0.05

part, covering 17.46% of the area (Fig. 5). These soils are particularly prone to erosion due to their low stability and infiltration capacity, leading to increased runoff and soil loss. The remaining 82.54% of the watershed, situated in the central and southern regions, exhibits medium erodibility.

The range of K factor values observed in the Ksob watershed is consistent with findings from other regions in Algeria, such as the Soummam watershed (Sahli et al., 2019) and the Wadi Medjerda watershed (Allaoui et al., 2023).

3.3 TOPOGRAPHIC FACTOR (LS FACTOR)

The topographic factor (LS factor) is a combined metric that includes two key elements: slope length and slope steepness. These factors are pivotal in determining the runoff and water erosion dynamics in the Ksob watershed. As both the length and steepness of the slope increase, the erosion rate also escalates due to the cumulative effect of runoff moving downslope. The LS factor map reveals values ranging from 0 to 42.66, with an average value of 0.146 (Fig. 6). This map distinctly mirrors the topographical characteristics of the watershed

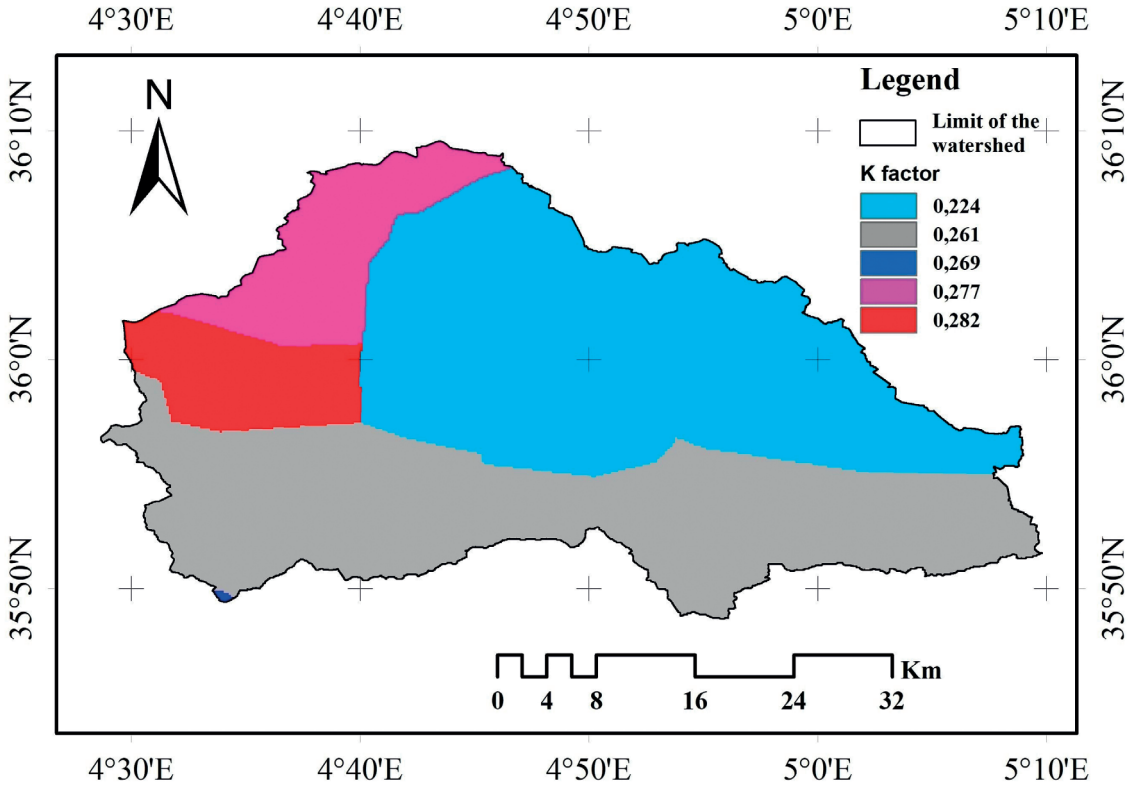

Fig. 5 - Spatial distribution of the erodibility factor (t h MJ^{-1} mm^{-1}).

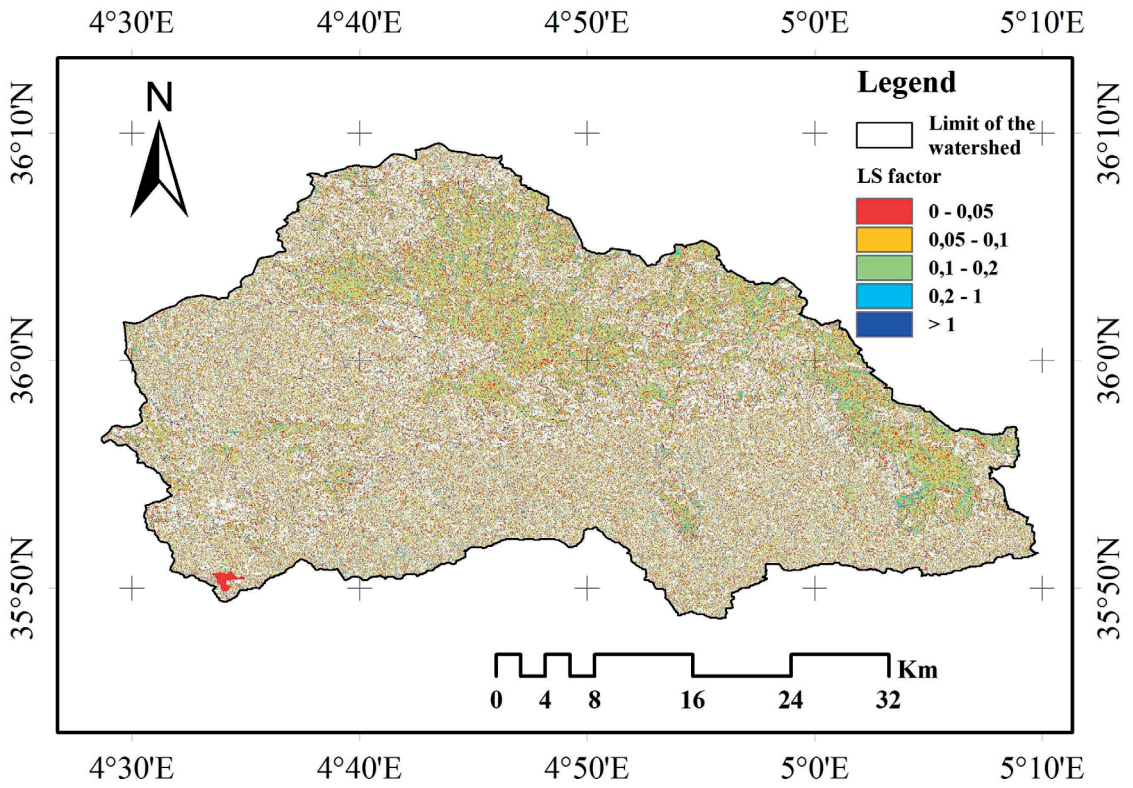

Fig. 6 - Spatial distribution of the topographic factor.

as depicted in Fig. 2. Areas with low LS values (less than 0.10) dominate 62.92% of the Ksob watershed, primarily located in the central and north-northeastern regions. These regions correspond to lower elevations, ranging between 600 to 1000 meters above sea level. Conversely, regions with higher LS values (greater than 0.2) indicate more rugged terrain characterized by steep slopes, with elevations reaching up to 1900 meters. These areas are limited in extent, covering no more than 13% of the watershed (refer to table 5). Such regions are particularly susceptible to water erosion due to the steep and rugged topography.

The range of LS factor values observed in the Ksob watershed aligns with findings from other regions in Algeria, such as the Wadi Sahouat basin (Toubal et al., 2018) and the Saf Saf watershed (Khanchoul et al., 2022).

Tab. 5 -Distribution of LS Factor classes in the Ksob watershed.

Classes of *LS*	Area (km²)	Area (%)
0-0.05	557.13	39.29
0.05-0.1	335.07	23.63
0.1-0.2	345.57	24.37
0.2-1	156.55	1.04
> 1	23.68	1.67
Total	1418.00	100.00

3.4. CROP MANAGEMENT (C FACTOR)

The C factor represents the influence of vegetation cover, crop residues, and land management practices on minimizing soil erosion. It quantifies how these factors collectively affect the rate of erosion. Vegetation indices derived from satellite data have proven to be effective proxies for assessing land cover in large basins and have been applied in various regions (Tanyas et al., 2015; Benavidez et al., 2018). In light of the results derived from these satellite-based indices and the C factor classification (refer to table 2), six distinct land cover classes were delineated within the watershed, which is predominantly composed of vegetation and rangeland.

The estimated C factor values range from 0 to 1, reflecting the degree of protection provided by vegetation cover against soil erosion. Over the period from 2017 to 2023, the interannual average C factor was calculated to be 0.654. This value indicates a moderate level of vegetation cover in the Ksob watershed (Fig. 7).

The spatial distribution analysis of the C factor over the period from 2017 to 2023, reveals significant trends in the watershed area. A key observation highlights that the majority of the watershed area has a relatively low level of vegetation, coupled with an increased susceptibility to water erosion, especially during the months of July and October, when the C factor often exceeds 0.7. This observation is particularly relevant in a semi-arid context, where rainfall is limited and temperatures are high during these periods. These meteorological conditions contribute to a reduction in vegetation cover and an

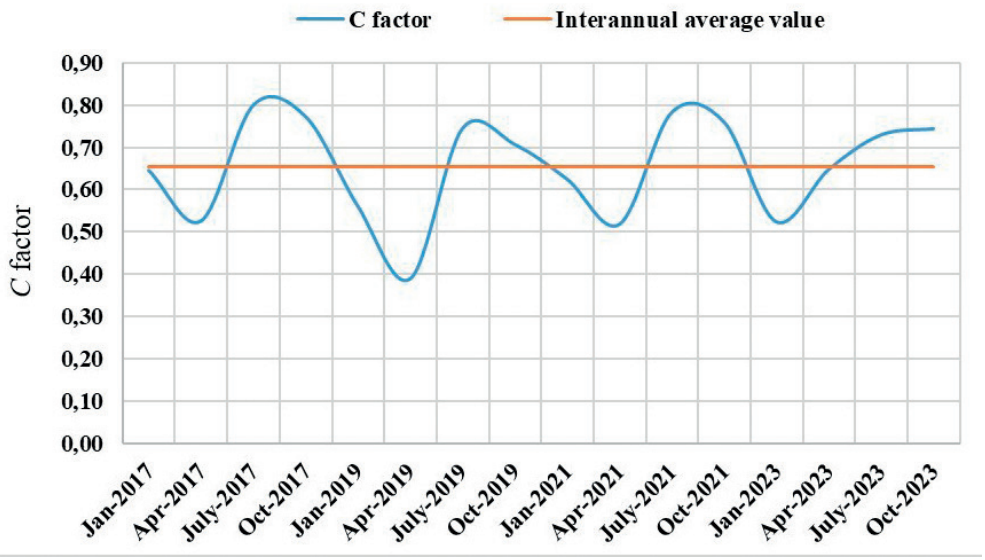

Fig. 7 - Interannual spatial distribution of the *C* factor.

increase in soil exposure to water erosion.

In contrast, an analysis of the months of January and April shows lower C factor values, averaging around 0.51. This finding suggests an increased vegetation development during these periods. Specifically, the low value of the C factor in January and April can be attributed to increased vegetation growth, especially due to the conversion of rangeland into vegetated land. This change in vegetation cover indicates potential land restoration efforts or agricultural practices conducive to vegetation growth, which could help reduce the region's vulnerability to water erosion.

3.4.1. Land use changes

Fig. 8 illustrates the different land use cover and their evolution in the study area between 2017 and 2023, while table 6 presents the data on LULC changes. Historically, rangeland has been the predominant land use type in the watershed, accounting for over 50% of the total area. Vegetation, primarily located in the northwestern and southeastern parts of the study area, constitutes the second most significant land use type, covering 31% of the total area. Together, these two land use types encompass approximately 81% of the total area. In contrast, trees, water bodies, urban areas, and bare land account for 8%, 3%, 5%, and 2% of the total area, respectively. The land use cover in the study area has experienced significant changes in recent years.

Over the years, the ratio of cultivated land has risen steadily, from 25.39% in 2017 to 33.74% in 2019, reaching 35.84% in 2023. At the same time, the land area has also increased, from 360.08 km^2 in 2017 to 508.21 km^2 in 2023. This growth is mainly due to land reclamation and the recovery of rangeland and unused land. In contrast, the proportion of rangeland will continue to decrease, from 57.81% in 2017 to 47.07% in 2023, with the area decreasing from 819.68 km^2 in 2017 to 667.49 km^2 in 2023, including rangeland recovery and reforestation efforts. The proportion of urban areas increased from 3.88% in 2017 to 5.07% in 2023, with an area that increased from 55.02 km^2 in 2017 to 71.90 km^2 in 2023, reflecting rapid economic development and increasing urbanization in central Algeria. The proportion of water areas varies significantly over this period, which can be explained by climate change and rainfall variability. On the other hand, tree cover and bare land have changed little.

3.5. CONSERVATION SUPPORT PRACTICE (P FACTOR)

The conservation practices P factor assesses the effectiveness of measures aimed at reducing surface runoff and soil erosion (Wischmeier and Smith, 1978). Typically, P factor values range from 0 to 1, with lower values indicating more effective erosion control. However, in the Ksob watershed, the absence of widespread anti-erosion infrastructure and cultivation practices results in minimal impact on erosion reduction. Consequently, a P factor value of 1 has been assigned across the entire watershed, reflecting the lack of effective erosion control measures. This approach is consistent with practices used by other Algerian researchers in similar soil erosion studies (Bouhadeb et al., 2015; Bensekhria and Bouhata, 2022).

3.6. ESTIMATION OF ANNUAL SOIL EROSION (A) USING RUSLE MODEL

Using the generated RUSLE factor maps, the average annual soil loss for the Ksob watershed was estimated for the years 2017 to 2023. The statistical analysis of soil loss during this period is presented in table 7. Results indicate that the estimated average annual soil loss increased from 9.06 t ha^{-1} yr^{-1} in 2017 to 10.08 t ha^{-1} yr^{-1} in 2023, marking an 11.21% rise in soil loss over the study period. This upward trend in soil erosion can be linked to various

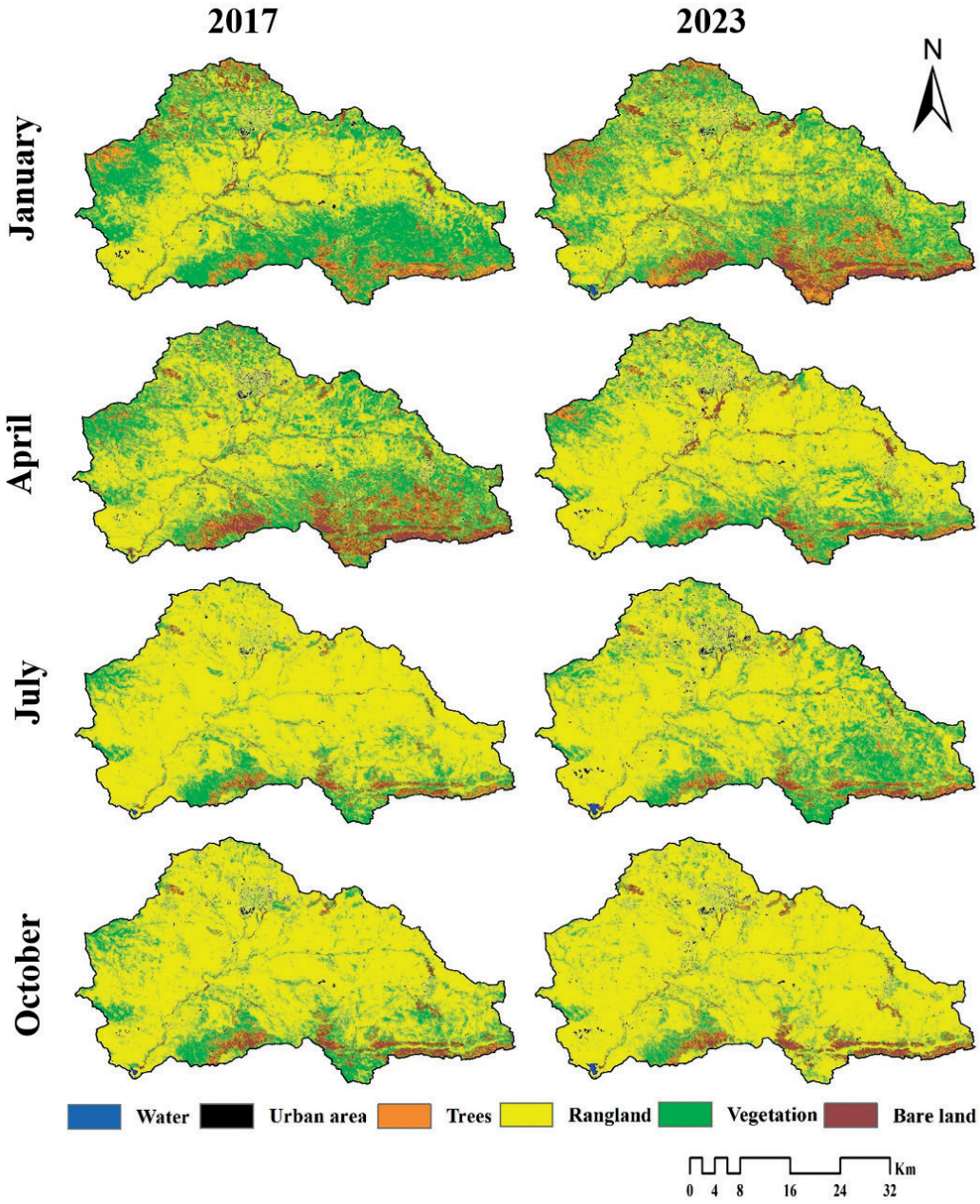

Fig. 8 - Spatial distribution and seasonal changes in the vegetation cover factor.

factors, including land use changes, climatic fluctuations, and other human activities.

The analysis of the area and soil erosion classes revealed notable changes in the Ksob watershed from 2017 to 2023. In 2017, the distribution of erosion classes was as follows: very low (40.26%), low (32.04%), moderate (20.98%), high (4.47%), and very high (2.25%). By 2023, the distribution had shifted to very low (35.99%), low (33.46%), moderate (23.19%), high (4.82%), and very high (2.55%) (Tab. 8, Fig. 9).

The results indicate that the Ksob watershed is generally characterized by mean erosion rates similar to Mediterranean basins (Lupia Palmieri et al., 1995). The most significant changes occurred in the very low, moderate, and very high soil erosion classes, while the low erosion class experienced the least change. The predominant erosion classes in the watershed, accounting for approximately 70% of the study area, are categorized as very low and low erosion classes.

These changes highlight a slight decline in the very low erosion class and a rise in the moderate and very high erosion classes, suggesting a trend towards greater soil erosion over time.

The erosion rates obtained in this study fall within the same range as those reported in previous research on other watersheds in Algeria, notably by Toubal et al. (2018). These findings are also comparable to results observed in Mediterranean and European regions where similar studies have been conducted. For example, in Italy, studies by Lupia Palmieri et al. (1998, 2001) revealed

Tab. 6 - Area of land use changes between 2017 and 2023 in the Ksob watershed.

Land use type	2017		2019		2021		2023		E1	E2	E3	E4
	(Km^2)	(%)	(Km^2)	(%)	(Km^2)	(%)	(Km^2)	(%)	(%)	(%)	(%)	(%)
Water	34.33	2.42	99.47	7.01	39.20	2.76	19.07	1.34	189.73	-60.59	-51.35	-44.45
Urban area	55.02	3.88	66.36	4.68	67.83	4.78	71.90	5.07	20.62	2.20	6.00	30.68
Trees	103.64	7.31	126.63	8.93	92.41	6.52	128.81	9.08	22.18	-27.03	39.40	24.29
Vegetation	360.08	25.39	478.36	33.74	433.23	30.55	508.21	35.84	32.85	-9.44	17.31	41.14
Rangland	819.68	57.81	630.83	44.49	771.20	54.39	667.49	47.07	-23.04	22.25	-13.45	-18.57
Bare land	45.25	3.19	16.35	1.15	14.14	1.00	22.51	1.59	-63.88	-13.51	59.24	-50,25

$E = 100 \times (area_{j+1} - area_j)/area_j$, j: is the stands for the year in various time frames.
E1 (2017-2019), E2 (2019-2021), E3 (2021-2023) and E4 (2017-2023).

Tab. 7 - Statistics parameters of soil loss rate (t ha^{-1} yr^{-1}).

Parameter	Soil loss 2017	Soil loss 2019	Soil loss 2021	Soil loss 2023	E1 (%)	E2 (%)	E3 (%)	E4 (%)
Minimum	0.00	0.00	0.00	0.00				
Maximum	309.23	286.38	299.23	302.66				
Average	9.06	8.63	9.78	10.08	-4.76	13.34	3.02	11.21
Ecartype	18.31	16.49	16.70	19.05				
CV	2.02	1.82	1.84	2.10				

Tab. 8 - Area of soil erosion class changes in the Ksob watershed.

Soil erosion classes	2017		2019		2021		2023		E1	E2	E3	E4
	(Km^2)	(%)	(Km^2)	(%)	(Km^2)	(%)	(Km^2)	(%)	(%)	(%)	(%)	(%)
Very low	570.84	40.26	596.95	42.10	532.56	37.56	510.40	35.99	4.57	-10.79	-4.16	-10.59
Low	454.34	32.04	461.25	32.53	466.04	32.87	474.42	33.46	1.52	1.04	1.80	4.42
Moderate	297.51	20.98	272.81	19.24	317.37	22.38	328.78	23.19	-8.30	16.33	3.60	10.51
High	63.41	4.47	56.80	4.01	67.05	4.73	68.29	4.82	-10.44	18.06	1.85	7.69
Very high	31.89	2.25	30.20	2.13	34.98	2.47	36.11	2.55	-5.33	15.86	3.23	13.22
Total	1418.00	100.00	1418.00	100.00	1418.00	100.00	1418.00	100.00				

comparable erosion rates under similar geographic and climatic conditions. Likewise, in Portugal, research by Ferreira et al. (2015) and, in Tunisia, studies by Gaubi et al. (2017) confirm similar erosion rate values, underscoring common dynamics in Mediterranean regions. These comparisons indicate that the erosive processes observed in the Ksob basin align with general trends in Mediterranean areas.

The spatial distributions of the Ksob watershed's predicted seasonal soil loss rates in 2017 and 2023 are shown in figure 10. In 2017, the months from July to October (corresponding to the summer and autumn seasons) were identified as experiencing the highest erosion rates, with monthly average soil loss rates exceeding 11 t ha^{-1} yr^{-1}. Conversely, the least soil erosion was observed during April (spring season), with an average monthly rate of 5.95 t ha^{-1} yr^{-1}. The regions most impacted by soil erosion were predominantly situated in the northern and eastern areas of the watershed. These regions consist of barren mountainous land, which is highly susceptible to erosion due to precipitation in the absence of vegetation cover.

In 2023, the months of April through October showed the highest impact of erosion, with average monthly soil loss rates exceeding 10 t ha^{-1} yr^{-1}. The minimal influence of soil loss was observed in January (winter season), with

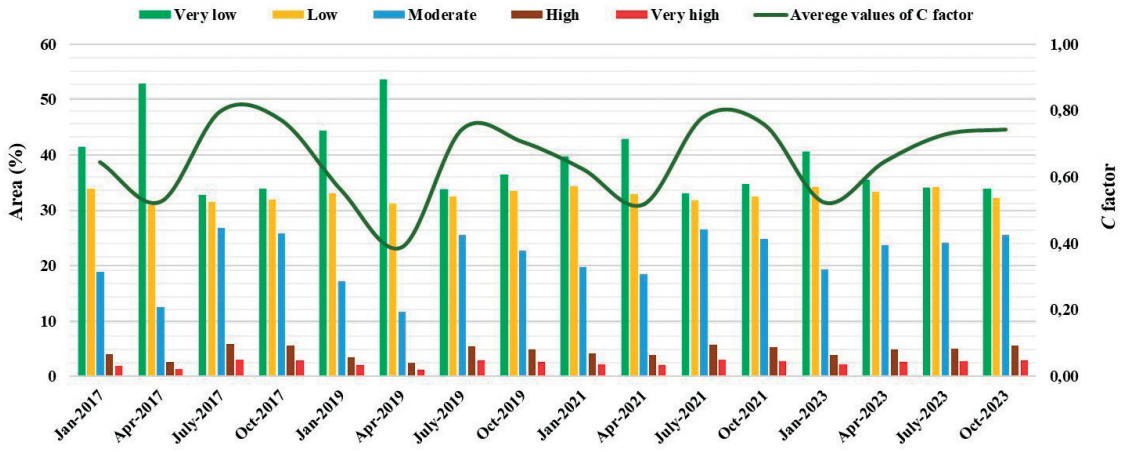

Fig. 9 - Changes in soil erosion surface class and C factor between 2017 and 2023.

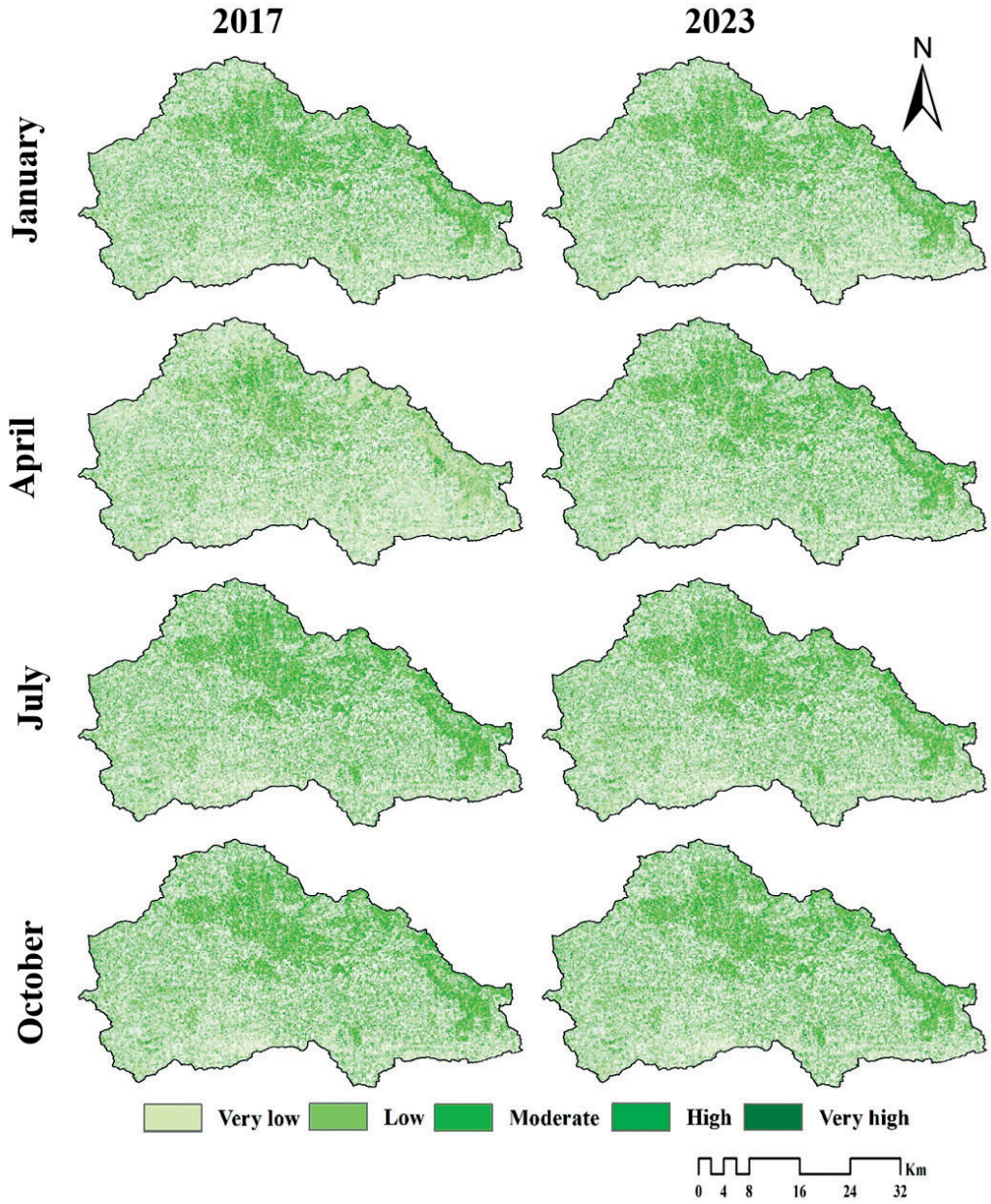

Fig. 10 - Spatial distribution and seasonal changes in soil loss rates (t ha^{-1} yr^{-1}).

an average monthly rate of 8.69 t ha^{-1} yr^{-1}. The regions most affected by soil loss were consistent with the findings from 2017, primarily concentrated in the northern and eastern areas of the watershed.

Many authors have highlighted the major impact of soil erosion during periods of heavy rainfall, especially toward the end of spring and the beginning of summer. For instance, Papy and Douyer (1991) identified this phenomenon in northwestern Europe, and Vandaele et al., (1995) observed similar results in Belgium. However, in the case of the Ksob watershed, data analysis reveals that erosion rates are particularly high in autumn and summer, exceeding those recorded in spring and winter. This difference could be attributed to the region's specific climatic and hydrological characteristics (Mediterranean zone), where autumn and summer rainfall, often in the form of intense downpours, lead to increased runoff and erosive force. These observations underscore a shift in the seasonal distribution of erosion, with a broader period of heightened erosion risk in 2023 compared to 2017. The continued susceptibility of the western-southern and central areas of the watershed underscores the necessity for specific soil conservation strategies aimed at alleviating ongoing soil erosion and degradation in these regions.

Seasonal variations in the *C* factor relative to the corresponding soil loss rate have been graphically represented in figure 11 to evaluate their influence on soil erosion. The results indicate a clear relationship between vegetation cover and erosion rate. When vegetation cover is dense (low *C* factor values), the erosion rate decreases. Conversely, when vegetation cover is sparse (high *C* factor values), the erosion rate increases.

The analysis shows that the summer and autumn seasons are particularly erosive compared to the winter and spring seasons. This pattern can be explained by the seasonal decrease or absence of vegetation cover during the warmer months, which increases soil exposure and susceptibility to erosion. During winter and spring, increased vegetation cover helps protect the soil, resulting in lower erosion rates. These findings underscore the critical role of vegetation in mitigating soil erosion. During periods of low vegetation cover, soil conservation measures such as mulching and cover cropping could be particularly beneficial in reducing soil loss. Furthermore, understanding these seasonal dynamics can inform the timing and implementation of conservation practices to maximize their effectiveness throughout the year. The annual variation of the soil loss rate concerning the different LULC classes has been represented in figure 12.

The findings of this study indicate that the most significant areas of soil loss are located in vegetated lands and mountainous regions, collectively accounting for over 50% of the watershed area. From 2017 to 2023, soil loss in the study area has intensified, particularly in the northern and southeastern mountainous regions, where forest soil loss has markedly increased. Overall, soil loss on cultivated land remains high, with the most severe erosion occurring on rangeland.

Several factors have contributed to the increase in soil loss observed between 2017 and 2023. One primary cause is the decrease in water bodies, which leads to less soil moisture and higher susceptibility to erosion. Water bodies have a crucial role to play in preserving soil stability and moisture. Their reduction has left large areas of soil dry and more susceptible to erosion. Additionally, the expansion of urban areas has disrupted the natural landscape. Urbanization often leads to the removal of vegetation and the compaction of soil, which reduces its ability to absorb water. This increases surface runoff and accelerates erosion.

The overexploitation of land has also significantly contributed to the increase in soil loss. Intensive agricultural practices, deforestation, and the conversion of land for development have degraded large areas, turning

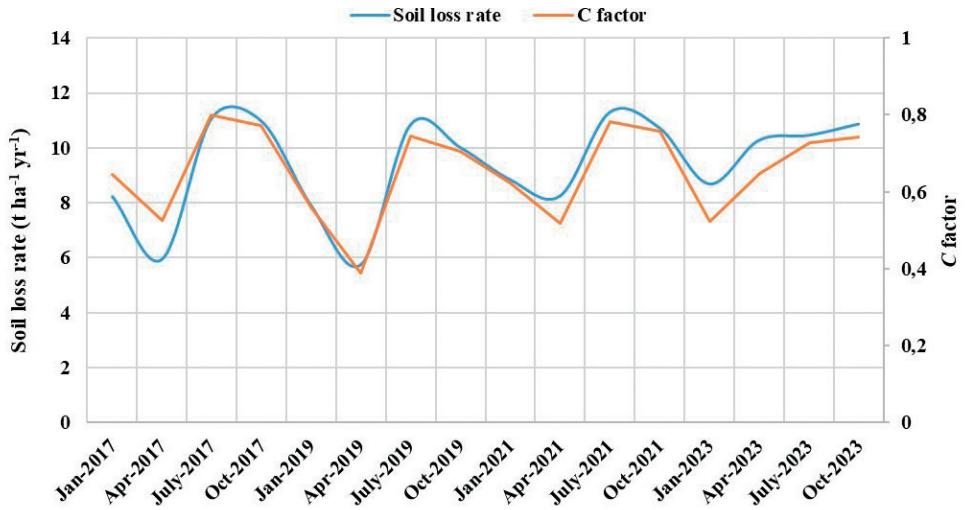

Fig. 11 - Seasonal variations in the C factor relative to the corresponding soil loss rate.

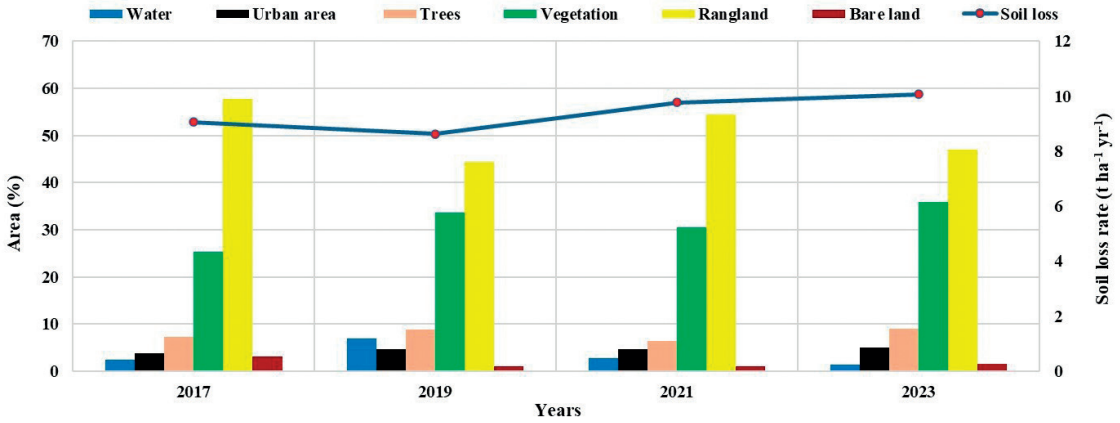

Fig. 12 - Annual variation of the soil loss rate concerning the different LULC classes.

them into unusable land such as sand and salt soils. This degradation destroys surface vegetation, which is essential for protecting soil from erosion. Without vegetation, the soil becomes loose and easily eroded by wind and water.

4. CONCLUSION

Soil erosion is a natural process that fluctuates over time, significantly influenced by variations in conditioning factors such as precipitation and, notably, vegetation cover. In this context, the present study examined seasonal and interannual variations in the *C* factor to determine soil loss in the Ksob watershed from 2017 to 2023. By using an empirical model such as RUSLE and high-resolution data (10x10 m) for the *C* and *R* factors, the study was able to obtain accurate results. Variations in the *C* factor, related to vegetation cover, were shown to have a significant impact on soil loss estimates. A decrease in vegetation cover, indicated by high values of the *C* factor, leads to increased erosion rates, whereas dense vegetation cover, indicated by low values of the *C* factor, helps to mitigate erosion. During the study period, the proportion of cultivated land grew significantly, rising from 25.39% in 2017 to 35.84% in 2023. Concurrently, the average annual soil erosion rate in the Ksob watershed escalated by 11.21%, increasing from 9.06 t ha^{-1} yr^{-1} in 2017 to 10.08 t ha^{-1} yr^{-1} in 2023. This increase can be attributed to several factors, including declining water bodies and the expansion of urban areas.

The Ksob watershed has experienced significant changes in erosion classes between 2017 and 2023. The results indicate that the most significant changes occurred in the very low, medium, and very high erosion classes, with the very low and low erosion classes dominating, representing approximately 70% of the total area. It was observed that the summer and autumn seasons are the most erosive, with average monthly soil loss rates exceeding 10 t ha^{-1} yr^{-1}. In contrast, minimal erosion is observed in the spring.

To assess the impact of seasonal variations in the *C* factor on soil loss rates, a comparative analysis was conducted in this study using a comparison graph. The results show a clear relationship between vegetation cover and erosion rate: when vegetation cover is dense (low *C* factor values), the erosion rate decreases. Conversely, when vegetation cover is sparse (high values of factor *C*), the erosion rate increases.

The critical necessity for focused soil conservation measures in the most impacted areas, rangeland and mountainous regions, in particular, is highlighted by the spatial analysis of erosion. Reforestation, contour farming, and terrace construction are a few techniques that can be used to stabilize the soil and lessen erosion. To reduce future soil erosion, it is also essential to address the sources of land degradation, such as overexploitation and inappropriate land use.

The study concludes by emphasizing how critical it is to comprehend the causes of soil erosion and put into practice practical soil conservation measures. The sustainability of land use practices and watersheds is contingent upon our capacity to efficiently control and alleviate soil erosion.

ACKNOWLEDGEMENTS - The Authors are very thankful to the anonymous reviewer, Prof. M. Del Monte, and the Edfitor-in-Chief for their careful and meticulous reading of the manuscript. We sincerely appreciate all valuable comments and suggestions, which have helped us to improve the quality of the article.

Statements and Declarations

Funding

The authors declare that no funds, grants, or other support were received during the preparation of this manuscript.

Competing Interests

The authors have no relevant financial or non-financial interests to disclose.

Author Contributions

All authors contributed to the study conception and design. Data collection and analysis were performed by

[Fouad Sakhraoui] and [Mahmoud Hasbaia]. All authors read and approved the final manuscript.

REFERENCES

Allaoui K., Mansouri R., Dorbani M., 2023. Soil erosion estimation of Wadi Medjerda in Algeria using the revised universal soil loss equation (RUSLE) through GIS" selected scientific papers. Journal of Civil Engineering 18.

Al Rammahi A.H.J., Khassaf S.I., 2018. Estimation of soil erodibility factor in rusle equation for euphrates river watershed using gis. International Journal of GEOMATE 14, 164-169.

Arnold J.G., Srinivasan R., Muttiah R.S., Williams J.R., 1998. Large area hydrological modelling and assessment part I: model development. Journal of the American Water Resources Association 34, 73-89.

Atoma H., Suryabhagavan K.V., Balakrishnan M., 2020. Soil erosion assessment using RUSLE model and GIS in Huluka watershed, Central Ethiopia. Sustainable Water Resources Management 6, 12.

Baskan O., 2021. Analysis of spatial and temporal changes of RUSLE-K soil erodibility factor in semi-arid areas in two different periods by conditional simulation. Archives of Agronomy and Soil Science 68, 1698-1710.

Belasri A., Lakhouili A., 2016. Estimation of Soil Erosion Risk Using the Universal Soil Loss Equation (USLE) and Geo-Information Technology in Oued El Makhazine Watershed, Morocco. Journal of Geographic Information System 8, 98-107.

Belkendil A., Habi M., Boutkhil M., Bouzouina O., Boufeldja S., 2018. Using multi–criteria evaluation (MCE): analytical hierarchy process (AHP) in investigation of erosion phenomenon in arid zones (case study: watershed of Bechar, Southwest of Algeria). Cinq Continents 8, 99-117.

Benavidez R., Jackson B., Maxwell D., Norton K., 2018. A review of the (revised) universal soil loss equation ((R) USLE): With a view to increasing its global applicability and improving soil loss estimates. Hydrology and Earth System Sciences 22, 6059-6086.

Benchettouh A., Kouri L., Jebari S., 2017. Spatial estimation of soil erosion risk using RUSLE/GIS techniques and practices conservation suggested for reducing soil erosion in Wadi Mina watershed (northwest, Algeria). Arabian Journal of Geosciences 10, 79.

Benkadja R., Boussag F., Benkadja A., 2015. Identification et évaluation du risque d'érosion sur le bassin versant du K'sob (Est Algérien) (Identification and assessment of erosion risk in the K'sob watershed (eastern Algeria)). Bulletin of Engineering Geology and the Environment 74, 91-102.

Bensekhria A., Bouhata R., 2022. Assessment and mapping soil water erosion using RUSLE approach and GIS tools: case of Oued el-Hai Watershed, Aurès West, Northeastern of Algeria. ISPRS International Journal of Geo-Information 11, 84.

Bollati I., Vergari F., Del Monte M., Pelfini M., 2016. Multitemporal dendrogeomorphological analysis of slope instability in upper Orcia Valley (Southern Tuscany, Italy). Geografia Fisica e Dinamica Quaternaria 39, 105-120.

Bouhadeb C.E., Menani M.R., Bouguerra H., Derdous O., 2018. Assessing soil loss using GIS based RUSLE methodology. Case of the Bou Namoussa watershed-North-East of Algeria. Journal of Water and Land Development 36, 27-35.

Chaves MED, Picoli MCA, Sanches ID, 2020. Recent Application of Landsat 8/OLI and Sentinel-2/MSI for land use and land cover mapping: a systematic review. Remote Sensing 12, 3062.

Chang T.J., Zhou H., Guan Y., 2016. Applications of erosion hotspots for watershed investigation in the Appalachian Hills of the United States. Journal of Irrigation and Drainage Engineering 142, 04015057.

Damian B., Rafał W., 2023. Evaluation of methods for determining the LS index at different resolutions for soil erosion modeling using the RUSLE method. Polish Journal of Agronomy 52, 110-122.

Dechen SCF, Telles TS, Guimarães MDF, Maria ICD, 2015. Perdas e custos associados à erosão hídrica em função de taxas de cobertura do solo [Losses and costs associated with water erosion depending on soil cover rates]. Bragantia 74, 224-233.

Degife A., Worku H., Gizaw S., 2021. Environmental implications of soil erosion and sediment yield in Lake Hawassa watershed, south-central Ethiopia. Environmental Systems Research 10, 28.

Diodato N., 2004. Estimating RUSLE's rainfall factor in the part of Italy with a Mediterranean rainfall regime. Hydrology and Earth System Sciences 8, 103-107.

Diodato N., 2005. Geostatistical uncertainty modelling for the environmental hazard assessment during single erosive rainstorm events. Environmental Monitoring and Assessment 105, 25-42.

Durigon V.L., Carvalho D.F., Antunes M.A.H., Oliveira P.T.S., Fernandes M.M., 2014. NDVI time series for monitoring RUSLE cover management factor in a tropical watershed. International Journal of Remote Sensing 35, 441-453.

Fernández C., Vega J.A., 2016. Evaluation of RUSLE and PESERA models for predicting soil erosion losses in the first year after wildfire in NW Spain. Geoderma 273, 64-72.

Ferreira V., Panagopoulos T., Cakulab A., Andradea R., Arvela A., 2015. Predicting soil erosion after land use changes for irrigating agriculture in a large reservoir of southern Portugal. Agriculture and Agricultural Science Procedia 4, 40-49.

Food and Agriculture Organization (FAO), 2012. Harmonized World Soil Database. FAO, Rome, Italy and IIASA, Laxenburg, Austria.

Gaubi I., Chaabani A., Ben Mammou A., Hamza M.H., 2017. A GIS-based soil erosion prediction using the revised universal soil loss equation (RUSLE) (Lebna watershed, Cap Bon, Tunisia). Natural Hazards 86, 219-239.

Gayen A., Saha S., Pourghasemi H.R., 2020. Soil erosion assessment using RUSLE model and its validation by FR probability model. Geocarto International 35, 1750-1768.

Gemechu E.D., Helbig C., Sonnemann G., Thorenz A., Tuma A., 2016. Import-based indicator for the geopolitical supply risk of raw materials in life cycle sustainability sssessments.

Journal of Industrial Ecology 20, 154-165.

Guerra C.A., Maes J., Geijzendorffer I., Metzger M.J., 2016. An assessment of soil erosion prevention by vegetation in Mediterranean Europe: Current trends of ecosystem service provision. Ecological Indicators 60, 213-222.

Gwapedza D., Nyamela N., Hughes DA, Slaughter AR, Mantel SK, Waal B., 2021. Prediction of sediment yield of the Inxu River catchment (South Africa) using the MUSLE. International Soil and Water Conservation Research 9, 37-48.

Khanchoul K., Boukhrissa Z.E.A., Othmani O., 2022. Spatial pattern of soil erosion using RUSLE model and GIS software at the Saf Saf watershed, Algeria. Acta Geographica Debrecina Landscape & Environment 16, 31-47.

Koirala P., Thakuri S., Joshi S., Chauhan R., 2019. Estimation of soil erosion in Nepal Using a RUSLE Modeling and geospatial tool. Geosciences 9, 147.

Lillesand T.M., Kiefer R.W., 2000. Remote Sensing and Image Interpretation. 4th edition. John Wiley and Sons, New York.

Liu H., Zhao W., Liu Y., 2020. Assessment on the Soil Retention Service of Water Erosion in the Nile River Basin Considering Vegetation Factor Variance from 1982 to 2013. Water 12, 2018.

Lupia Palmieri E., Ciccacci S., Civitelli G., Corda L., D'Alessandro L., Del Monte M., Fredi P., Pugliese F., 1995. Geomorfologia quantitativa e morfodinamica del territorio abruzzese: I-II bacino idrografico del Fiume Sinello. Geografia Fisica e Dinamica Quaternaria 18, 31-46.

Lupia Palmieri E., Centamore E., Ciccacci S., D'Alessandro L., Del Monte M., Fredi P., Pugliese F., 1998. Geomorfologia quantitativa e morfodinamica del Territorio abruzzese: II - II bacino idrografico del Fiume Tordino. Geografia Fisica e Dinamica Quaternaria 21, 113-129.

Lupia Palmieri E., Biasini A., Caputo C., Centamore E., Ciccacci S., Del Monte M., Fredi P., Pugliese F., 2001. Geomorfologia quantitativa e morfodinamica del Territorio abruzzese: I-II bacino idrografico del Fiume Tordino. Geografia Fisica e Dinamica Quaternaria 24, 157-176.

Mahleb A., Hadji R., Zahri F., Boudjellal R., Chibani A., Hamed Y., 2022. Water-borne erosion estimation using the revised universal soil loss equation (RUSLE) model over a semiarid watershed: Case study of Meskiana Catchment, Algerian-Tunisian Border. Geotechnical and Geological Engineering 40, 4217-4230.

Macedo P.M.S., Oliveira P.T.S., Antunes M.A.H., Durigon V.L., Fidalgo E.C.C., Carvalho D.F., 2021. New approach for obtaining the C-factor of RUSLE considering the seasonal effect of rainfalls on vegetation cover. International Soil and Water Conservation Research 9, 207-216.

Mazour M., Roose E., 2002. Influence de la couverture végétale sur le ruissellement et l'érosion des sols sur parcelles d'érosion dans des bassins versants du Nord-Ouest de l'Algérie. En: Techniques traditionnelles de GCES en milieu méditerranéen [Influence of vegetation cover on runoff and soil erosion on erosion plots in watersheds in north-western Algeria. In: Traditional techniques of GCES in the Mediterranean environment]. Bulletin Réseau Erosion 21, 320-330.

Meusburger K., Bänninger D., Alewell C., 2010. Estimating vegetation parameter for soil erosion assessment in an alpine catchment by means of QuickBird imagery. International Journal of Applied Earth Observation and Geoinformation 12, 201-207.

Mitasova H., Hofierka J., Zlocha M., Iverson L.R., 1996. Modelling topographic potential for erosion and deposition using GIS. International Journal of Geographical Information Systems 10, 629-641.

Molla T., Sisheber B., 2017. Estimating Soil erosion risk and evaluating erosion control measures for soil conservation planning at Koga Watershed in the Highlands of Ethiopia. Solid Earth 8, 13-25.

Morgan R.P.C., Quinton J.N., Smith R.E., Govers G., Poesen J.W.A., Auerswald K., Chisci G., Torri D., Styczen M.E., 1998. The european soil erosion model (EUROSEM): a dynamic approach for predicting sediment transport from fields and small catchments. Earth Surface Processes and Landforms 23, 527–544.

Morgan R.P.C., 2005. Soil Erosion and Conservation. 3rd edition. Blackwell, Oxford.

Neitsch S.L., Williams J.R., Arnold J.G., Kiniry J.R., 2011. Soil and Water Assessment Tool Theoretical Documentation. Texas Water Resources Institute, College Station, Texas 77843-2118.

Negese A., Fekadu E., Getnet H., 2021. Potential soil loss estimation and erosion-prone area prioritization using RUSLE, GIS, and Remote Sensing in Chereti Watershed, Northeastern Ethiopia. Air, Soil, and Water Research 14.

Nourizadeh M., Naghavi H., Omidvar E., 2024. The effect of land use and land cover changes on soil erosion in semi-arid areas using cloud-based google earth engine platform and GIS-based RUSLE model. Natural Hazards 120, 6901-6922.

Ochoa PA, Fries A., Mejia D., Burneo JI, Ruiz-Sinoga JD, Cerda A., 2016. Effects of climate, land cover and topography on soil erosion risk in a semiarid basin of the Andes. Catena 140, 31-42.

Papy F., Douyer C., 1991. Influence des 6tats de surface du territoire agricole sur le declenchement des inondations catastrophiques. Agronomie 11, 201-215.

Polidoro JC, Freitas PL, Hernani LC, Anjos LHCD, Rodrigues RDAR, Cesário FV, Ribeiro JL, 2021. Potential impact of plans and policies based on the principles of conservation agriculture on the control of soil erosion in Brazil. Land Degradation & Development 32, 3457-3468.

Phinzi K., Ngetar N.S., 2018. The assessment of water-borne erosion at catchment level using GIS-based RUSLE and remote sensing: A review International Soil and Water Conservation Research 7, 27-46.

Puente C., Olague G., Smith S.V., Bullock S.H., Hinojosa-Corona A., González Botello M.A., 2011. A genetic programming approach to estimate vegetation cover in the context of soil erosion assessment. Photogrammetric Engineering & Remote Sensing 14, 363-376.

Renard K.G., Foster G.R., Weesies G.A., McCool D.K., Yoder D.C., 1997. Predicting soil erosion by water: a guide to conservation planning with the Revised Universal Soil Loss Equation (RUSLE). Agriculture Handbook No. 703. USDA-

ARS, DC, Washington.

Rodrigues W.F., Costa I.G., 2021. Danos ambientais provocados por incêndios no Cerrado: uma análise entre os anos de 2004 e 2019 no Parque Nacional da Serra da Canastra-MG [Environmental damage caused by fires in the Cerrado: an analysis between 2004 and 2019 in the Serra da Canastra National Park-MG]. Ensaios de Geografia 7, 163-188.

Sahli Y., Mokhtari E., Merzouk B., Benoit L., Christophe V., Khodir M., 2019. Mapping surface water erosion potential in the Soummam watershed in Northeast Algeria with RUSLE model. Journal of Mountain Science 16, 1606-1615.

Sakhraoui F., Hasbaia M., 2023. Evaluation of the sensitivity of the RUSLE erosion model to rainfall erosivity: a case study of the Ksob watershed in central Algeria. Water Supply 23, 3262-3284.

Santana D.B., Bolleli T.M., Lense G.H.E., Silva L.F.P.M., Sestras P., Spalevic V., Mincato R.L., 2021. Estimate of water erosion in coffee growing areas in Serra da Mantiqueira, Minas Gerais State, Brazil. Agriculture and Forestry 67, 75-88.

Sharpley N.A., Williams R.J., 1990. EPIC-erosion/Productivity Impact Calculator I, Model Documentation. U.S. Department of Agriculture Technical Bulletin, Beltsville, MD, USA.

Sifi S., Aydi A., Bouamrane A., Zaghdoudi S., Gasmi M. 2024. Appraisal of soil erosion risk in northeastern Tunisia using geospatial data and integrated approach of RUSLE model and GIS. Journal of Earth System Science 133, 67.

Singh M.C., Sur K., Al-Ansari N., Arya P.K., Verma V.K., Malik A., 2023. GIS integrated RUSLE model-based soil loss estimation and watershed prioritization for land and water conservation aspects. Frontiers in Environmental Science 11, 1136243.

Sourn T., Pok S., Chou P., Nut N., Theng D., Prasad P.V.V., 2022. Assessment of Land Use and Land Cover Changes on Soil Erosion Using Remote Sensing, GIS and RUSLE Model: A Case Study of Battambang Province, Cambodia. Sustainability 14, 4066.

Tadesse L., Suryabhagavan KV, Sridhar G., Gizachew L., 2017. Land use and land cover changes and soil erosion in Yezat watershed, north western Ethiopia. International Soil and Water Conservation Research 5, 85-94.

Tanyas H., Kolat Ç., Süzen M.L., 2015. A new approach to estimate cover management factor of RUSLE and validation of RUSLE model in the watershed of Kartalkaya Dam. Journal of Hydrology 528, 584-598.

Toubal A.K., Achite M., Ouillon S., Dehni A., 2018. Soil erodibility mapping using the RUSLE model to prioritize erosion control in the Wadi Sahouat basin, North-West of Algeria. Environmental Monitoring and Assessment 190, 210.

Valkanou K., Karymbalis E., Bathrellos G., Skilodimou H., Tsanakas K., Papanastassiou D., Gaki-papanastassiou K., 2022. Soil loss potential assessment for natural and post-fire conditions in Evia Island, Greece. Geosciences 12, 367.

Van D.K.J., Jones R., Montanarella L., 2000. Soil erosion risk assessment in Europe. Office for Official Publications of the European Communities, Luxembourg.

Van Rompaey A.J.J., Verstraeten G., Van Oost K., Govers G., Poesen J., 2001. Modelling mean annual sediment yield using a distributed approach. Earth Surface Processes and Landforms 26, 1221-1236.

Vandaele K., Poesen J., 1995. Spatial and temporal patterns of soil erosion rates in an agricultural catchment, central Belgium. Catena 25, 213-226.

Vandekerckhove L., Poesen J., Oostwoud Wijdenes D., De Figueiredo T., 1998. Topographical thresholds for ephemeral gully initiation in intensively cultivated areas of the Mediterranean. Catena 33, 271-292.

Vergari F., Troiani F., Faulkner H., Del Monte M., Della Seta M., Ciccacci S., Fredi P., 2019. The use of the slope-area function to analyse process domains in complex badland landscapes. Earth Surface Processes and Landforms 44, 273-286.

Wang Q., Xu Y., Xu Y., Wu L., Wang Y., Han L., 2018. Spatial hydrological responses to land use and land cover changes in a typical catchment of the Yangtze River Delta region. Catena 170, 305-315.

Wischmeier W.H., Smith D.D., 1965. Predicting rainfall-erosion losses from cropland east of the Rocky Mountains. Guide for selection of practices for soil and water conservation, US Government Printing Office, Washington.

Wischmeier W.H., Smith D.D., 1978. Predicting rainfall erosion losses-a guide to conservation planning. Agricultural Handbook 282. USDA-ARS, USA.

Xu L.F., Xu X.G., Meng X.W., 2012. Risk assessment of soil erosion in different rainfall scenarios by RUSLE model coupled with Information Diffusion Model: A case study of Bohai Rim, China. Catena 100, 74-82.